ELSEVIER

Biophysical Chemistry 80 (1999) 69–83

Biophysical Chemistry

www.elsevier.nl/locate/bpc

Comparison of dynamic and integrated light-scattering techniques in the study of the interaction of *Candida rugosa* lipase with DPPC liposomes

Clara López-Amaya, Alejandro G. Marangoni*

Department of Food Science, University of Guelph, Guelph, Ontario, Canada N1G 2W1

Received 16 October 1998; received in revised form 8 April 1999; accepted 12 April 1999

Abstract

Dynamic light-scattering (DLS) and wide angle integrated light-scattering (WAILS) spectroscopies were evaluated in the study of binding of *Candida rugosa* lipase (CRL) with 1,2-dipalmitoyl-*sn*-glycero-3-phosphocholine (DPPC) liposomes. The use of cumulants analysis on DLS data allowed for the determination of general lipase–liposome-binding trends. Particle intensity distributions obtained from DLS data by a discrete inversion method revealed the different populations created upon lipase–liposome interactions. Using a discrete inversion technique on WAILS data, not only these populations could be differentiated but also accurate number distributions were obtained in short periods of time. Both DLS and WAILS are excellent tools for the study of lipase binding to lipid vesicles; however, care must be exercised in the analysis of the experimental data whenever particle size distributions are multimodal. The selection of the light scattering technique will depend on the information required.

Keywords: Lipase; Binding; Dynamic light-scattering; Integrated light-scattering; Lipase–liposome interactions; Protein–lipid interactions

1. Introduction

Lipases (EC 3.1.1.3) hydrolyze ester bonds in tri-acylglycerols to yield free fatty acids, di- and mono-acylglycerol and glycerol. These enzymes are widely distributed in nature and are produced by animals, plants and microorganisms. Among the microbial lipases *Candida rugosa* lipase (CRL) is one of the most widely used in industrial applications due to its high activity in ester synthesis [1–3], and in lipid hydrolysis [4,5].

Lipase and phospholipase natural substrates are insoluble in water and their activity is maxi-

* Corresponding author. Tel.: +1-519-824-4120 ext. 4340; fax: +1-519-824-6631.
E-mail address: amarango@foodsci.uoguelph.ca (A.G. Marangoni)

0301-4622/99/$ - see front matter
PII: S0301-4622(99)00062-9

mum only at the lipid–water interface. This unique property known as interfacial activation [6] may differ for each specific lipase [7]. The several hypotheses that have been proposed to explain the interfacial activation phenomenon can be classified into two categories: the substrate models and the enzyme models [8]. Substrate models describe interfacial activation as the result of changes in the substrate itself. Changes in substrate concentration, conformation/orientation, and the hydration-state at the interface may be involved in the process [9]. Enzyme models relate interfacial activation to a regulation of the catalytic power of the enzyme by the lipid–water interface. In this category, a model proposed by Verger et al. [10] is at present, the most generally accepted. A conformational change of the lipolytic enzyme upon interaction with interfaces [11] would induce a modification in the active site, triggering the high catalytic rates observed in substrate aggregates. The existence of an additional site in the enzyme, topographically and functionally distinct from the active site, responsible for the interaction between the enzyme and the substrate aggregate [10,12] is assumed. This region has been identified as the 'penetration site' [10], 'supersubstrate binding site' [12], and 'interface recognition site' (IRS) [6].

Although the amount of published work in the field of phospho(lipase) structure–function is prolific owing to its importance in medicine, mechanisms such as interfacial activation are still not completely understood. Studies on the nature of peptide- and phospholipase-vesicle or micelle interactions using a variety of techniques have been published. Fluorescence spectroscopy studies have allowed for the identification of the driving forces and the determination of dissociation constants for peptide–lipid [13,14] and phospholipase A_2-phospholipid bilayer [15] interactions. Fluorescence spectroscopy has also been used to determine stoichiometry and binding constants for lipoprotein–vesicle interactions [16]. The formation, stability and molecular weight of the complex formed between porcine pancreatic phospholipase A_2 and triglyceride–bile salt micelles has been studied by dynamic light scattering (DLS) spectroscopy, isothermal calorimetry and equilibrium gel filtration, respectively [17]. Moreover, the interaction of porcine pancreatic phospholipase A_2 (PA-2) with micelles of various single-chain phospholipid analogs was studied by UV absorption difference spectroscopy and light-scattering spectroscopy measurements [18]. The affinity of cobra venom phospholipase A_2 for mixed micelles (Triton X100-long chain phospholipids) has been determined by equilibrium gel filtration [19]. Integrated light scattering (ILS) and DLS have been used to monitor changes in vesicle radius as a result of incorporation of membrane-soluble peptide to vesicle lipid bilayers [20].

With respect to microbial lipases, a better understanding of interfacial binding is essential for the exploitation and control of lipase catalytic properties. The literature is full of reports on the industrial use of microbial lipases, but studies related to interfacial binding are scarce. The incorporation of CRL in polymer vesicles has been detected by fluorescence spectroscopy [21]. DLS and ILS spectroscopies can be used to obtain size distributions of particles between 0.01 and 2 mm ([13] and references therein). DLS has been previously used in the study of the interaction of *Rhizopus arrhizus* (RAL) with DOPG and DPPC liposomes. While binding of RAL to DOPG liposomes was not detected, binding of RAL to DPPC liposomes was monitored and affinity parameters for the interaction were calculated [22]. In the present investigation we have characterized the interaction of *Candida rugosa* lipase to DPPC liposomes under different conditions of pH, ionic strength and temperature using DLS and wide angle integrated light scattering (WAILS) spectroscopies. As well, a new method of DLS data analysis was assessed and compared to the traditional cumulants analysis. The results obtained were compared with those obtained by WAILS.

2. Light scattering theory

In DLS, the electric field autocorrelation function, $g^{(1)}(\tau)$, for monodisperse solutions (all particles are identical in size) where particles are

spherical particles is [23]:

$$g^{(1)}(\tau) = e^{-DQ_\tau^2} \tag{1}$$

where D is the diffusion coefficient of the scatterers, the scattering vector, Q, results from the difference of the scattered and the incident wave vectors (k_o–k_s) and τ is the time interval for displacement of the scattering particle. In practice, the 0 delay ($\tau = 0$) intercept is 'a' where $a \leq 1$. On the other hand, for a suspension that contains a distribution of scatterers $g^{(1)}(\tau)$ becomes a summation, with weightings, over all the sizes present,

$$\begin{aligned} g^{(1)}(\tau) &= a\left(\omega_1 e^{-D_1 Q^2 \tau} + \omega_2 e^{-D_2 Q^2 \tau} + \dots\right) \\ &= a \sum_{i=1}^{m} \omega_i e^{-D_1 Q^2 \tau} \end{aligned} \tag{2}$$

where ω_i corresponds to a weighting factor related to the relative abundance of particles of a size indexed by i, and m stands for the number of sizes. Having a continuous distribution of sizes Eq. (2) can be replaced by,

$$g^{(1)}(\tau) = a\int_0^\infty G(\Gamma) e^{-\Gamma\tau} d\Gamma \tag{3}$$

where $\Gamma = DQ^2$.

A complete Laplace inversion of Eq. (3) would generate the distribution of decay rates, $G(\Gamma)$, from which the particle sizes distribution can be determined using the Stokes–Einstein equation,

$$D = \frac{kT}{6\pi\eta R_h} \tag{4}$$

In the Stokes–Einstein equation k is Boltzmann's constant, T is the absolute temperature, η is the coefficient of viscosity of the medium, and R_h is the hydrodynamic radius of the particle. Such an inversion is called 'ill conditioned' because of its mathematical instability and because of the need of extremely high precision experimental data [23]. Consequently, less demanding alternative methods have been used, but with a corresponding reduction in the information obtained. Among them the most common one is called moments or cumulants analysis. This procedure consists in an expansion of $e^{-\Gamma\tau}$ about the mean value $e^{-\bar{\Gamma}\tau}$ [24],

$$\begin{aligned} e^{-\Gamma\tau} &= e^{-\bar{\Gamma}\tau} e^{(-(\Gamma-\bar{\Gamma})\tau)} \\ &= e^{-\bar{\Gamma}\tau}\left(1 - (\Gamma-\bar{\Gamma})\tau + \frac{(\Gamma-\bar{\Gamma})^2\tau^2}{2!}\right. \\ &\quad \left. - \frac{(\Gamma-\bar{\Gamma})^3\tau^3}{3!} + \dots\right) \end{aligned} \tag{5}$$

Which upon substitution into Eq. (3) and taking the logarithm yields [23],

$$\ln(g^{(1)}(\tau)) = \ln(a) - \bar{\Gamma}\tau + \frac{\mu_2}{2!} - \tau^2 - \frac{\mu_3}{3!}\tau^3 + \dots \tag{6}$$

The second moment, μ_2, corresponds to the variance since the first moment about the mean, μ_1, is always zero. Replacing $\tau = kt$, where k is the channel number and t is the sampling time (an instrumental setting), in Eq. (6),

$$\ln(g^{(1)}(\tau)) = A - Bk + Ck^2 - Dk^3 + \dots \tag{7}$$

where $A = \ln(a)$,

$$B = \bar{\Gamma}\tau = \frac{t}{(\bar{D}Q^2)} \quad \text{and} \quad C = \frac{\mu_2}{2!}t^2.$$

A least squares fit of the natural logarithm of $g^{(1)}(\tau)$ to a third order polynomial can be applied to obtain the coefficients. The average radius of the scatterers (assumed to be spherical) can be determined from B and Eq. (4) [23].

Other more sophisticated approaches to the inversion of Eq. (3) are variants of a discrete procedure in which,

$$\text{Var} = \left(g^{(1)}(\tau) - \sum^{m} \omega_m \exp(-\Gamma_m\tau)\right)^2 \tag{8}$$

is minimized with respect to the variables ω_m and Γ_m. The Γ_m are exponentially spaced in the method called exponential sampling [25] as shown in the following relation,

$$\Gamma_{m+1} = \Gamma_m \exp(\chi) \quad (9)$$

where the constant χ sets the initial spacing between the first two Γs. Morrison et al. [26] combined exponential sampling with non-negative least square (NNLS) procedures. In this method ω's are restricted to be positive. The set of ω's obtained corresponds to the amplitudes or relative weights tied to each of the Γs in the exponentials of Eq. (8). The amplitudes can be displayed in histogram form because each Γ has a corresponding r [23].

In the described methods, resulting histograms are intensity-weighted distributions where the amplitudes represent the amount of light scattered by each particle size, r and decay constant Γ. Inclusion of the relative scattering ability of each size in the distribution allows calculation of number distributions. This can be attained by including Rayleigh–Gans–Debye or Mie scattering factors in the sumation of Eq. (8), procedure that introduces spurious oscillations into the ω's. To surmount this problem, Hallett et al. [27] devised an extension of NNLS exponential sampling [26] which includes the use of triangles in Γ space rather than delta functions. Delta functions to triangle conversion and calculations of number distribution procedures are described in detail by Hallett et al. [27].

In ILS, to obtain the size distribution function, $G(r)$, of the vesicles, the following equation must be solved [20],

$$I(Q) = \int_0^\infty I(Q,r)_{TH} G(r) \mathrm{d}r \quad (10)$$

where $I(Q,r)_{TH}$ is the theoretical scattered intensity for coated spheres of radius r. As the inversion of this equation is ill-conditioned, a discrete non-negative least-squares fitting which includes a range and spacing of predetermined trial radii, is applied. The trial radii, between $r_{\min}$ and $r_{\max}$, are distributed geometrically,

$$r_n = r_{\min}\left[\left(\frac{r_{\max}}{r_{\min}}\right)^{1/m}\right]^{n-1} \quad (11)$$

where m is the total number of radii. The program minimizes var where,

$$\mathrm{var} = \left[I(Q) - \sum_{n=1}^{m} a_n I(Q,r_n)_{TH}\right]^2 \quad (12)$$

and where a_n represents the amplitude of a histogram and is constrained to be positive. The size distribution program uses a non-negative least-squares algorithm to calculate number distributions for hollow spherical shapes using Mie theory. The program outputs the fitted form of $I(Q)$ as a histogram and also provides information on the moments of the distribution [28].

3. Experimental procedures

3.1. Chemicals

Unless otherwise stated, chemicals were of reagent grade and were purchased from Merck (Toronto, Ontario, Canada).

3.2. Liposome preparation

Liposomes were prepared by extrusion essentially as described by Nayar et al. [29]. Thirty milligrams of 1,2-dipalmitoyl-*sn*-glycero-3-phosphocholine (DPPC) powder form (Avanti Polar-Lipids, Inc., Alabaster, AL, USA) were suspended in 1 ml of the buffer required for each experiment (0.1 M MOPS, pH 7.5; 0.1 M succinate, pH 5.0; 0.2 M NaCl, 0.1 M MOPS, pH 7.5 or 0.2 M NaCl, 0.1 M succinate, pH 5.0) followed by 1-min vortex mixing. DPPC suspensions were frozen and thawed 10 times in liquid N_2 and water bath at 52°C, respectively. The extrusion was performed 10 times at 160 p.s.i. and 52°C through two stacked polycarbonate filters (Nucleopore Corp., Pleasanton, CA, USA) of 100- or 200-nm pore size. The final concentration of the extruded vesicle preparations ($n = 3$) was 23.1 mg (S.D. = 1.2 mg) phospholipid/ml buffer, as determined by the procedure for phospholipid phosphorus analysis of Bartlett [30]. Vesicles were stored at 25°C for a maximum period of 72 h.

3.3. Candida rugosa lipase preparation

The extraction was performed on a suspension of 30 g of *Candida rugosa* lipase type VII, lyophilized form (Sigma, St Louis, MO, USA) dissolved in 100 ml of 25 mM Tris–HCl buffer, pH 7.5, following the procedure described by Veeraragavan and Gibbs [31]. The obtained dialyzate was changed for 3 days (12 h changes), centrifuged again, and filtered through a 0.22 mm pore membrane (Steril Acrodisc, Gelman Sciences). The resultant enzyme stock solution was stored at −40°C until use. Thawed enzyme was maintained for a maximum of 1 week at 4°C. Protein concentration was measured by the method of Bradford [32] using BSA as standard. Three different enzyme batches with protein concentrations of 1.17, 1.35, and 0.62 mg/ml were used.

3.4. Enzyme activity

Enzyme activity was determined by a modification of the emulsified substrate assay of Veeraragavan and Gibbs [31]. An emulsion was obtained by mixing 0.22 mg/ml olive oil, 1% gum arabic, and 50 mM phosphate buffer, pH 6.0, using a Polytron homogenizer (Tekmar, Cincinnati, OH, USA) at high speed for 5 min. In a 10-ml glass vial, 0.45 ml of the emulsion and 0.1 ml of the enzyme sample were mixed and incubated in a water bath at 40°C for 1 h. For the fatty acid determination, basically the method of Kwon and Rhee [33] was followed. The enzyme reaction in the emulsion was stopped by adding 0.5 ml of 6 N HCl and 5 ml of isooctane, mixing very well (using a vortex at high speed), and boiling the mixture for 5 min. When the vials had cooled down on ice to room temperature, 4 ml of the upper layer were transferred to a clean 10 ml glass vial, and 1 ml of cupric acetate–pyridine reagent was added; the two phases formed were vortexed for 1 min at high speed and allowed to sit for 10 min. The upper phase was removed and its absorbance was read at 715 nm. The amount of free fatty acids was determined from an oleic acid standard curve in the range of 2–50 mmol/5 ml isooctane [33].

3.5. Phospholipid hydrolysis

To assess the hydrolysis of phospholipid by lipase, liposomes were prepared as described in the liposome preparation in Section 3.2 and the dispersion was diluted with buffer to 4 ml, followed by mixing. Two hundred millilitres of the enzyme was added and the reaction mixture was incubated in a water bath at 35°C. At the beginning of the reaction and after 3-, 6-, 12-, 19-, 24- and 48 h periods, 200 ml aliquots were withdrawn and assayed for free fatty acids by the procedure described above for olive oil emulsions. No hydrolysis was detected in the described system. Other phospholipids such as DOPC, DOPG and DPPG (Avanti Polar-Lipids, Inc., Alabaster, AL, USA) and other lipases such as *Rhizopus arrhizus*, *Mucor* spp., *Geotrichum* spp. and *Candida rugosa* (Amano) were evaluated for hydrolysis and the results were negative as well.

3.6. Dynamic light-scattering (DLS)

A Malvern 4700 light scattering spectrometer (Malvern Instruments, Malvern, UK) was used for DLS experiments. Aliquots of DPPC liposome suspension (60 μl and 100 μl for extrusion done with 200 nm and 100 nm pore filters, respectively) in 0.1 M succinate buffer, pH 5.0, and in 0.1 M phosphate buffer, pH 7.5, without NaCl and with 0.2 M or 1.0 M NaCl were mixed with CRL (10–125 ml) and incubated at 25, 35, or 45°C for 15 min. After the incubation period, the mixtures were diluted (to a final volume of 3 ml and 2.7 ml for extrusions done with 200 nm and 100 nm pore filter membranes, respectively) with the buffer previously used for vesicle preparation. Protein concentrations of 6.5×10^{-8} M, 1.3×10^{-7} M, 2.3×10^{-7} M, 3.3×10^{-7} M, 3.9×10^{-7} M, 4.9×10^{-7} M, 5.9×10^{-7} M, 6.5×10^{-7} M or 8.1×10^{-7} M and a phospholipid concentration of 6.3×10^{-4} M were present in the final volume mixture. After a 5-min period of maintaining the sample in the sample holder to let the system reach the required temperature, a He–Ne laser (633 nm wavelength) was focused onto the sample, and scattered light was detected at a scattering angle of 90°. The sample time was 25 ms. In

order to verify the laser alignment, 135-nm polystyrene latex microspheres (Duke Scientific Corp., Palo Alto, CA, USA) were measured before each experiment. Using software provided by Malvern the diffusion coefficients were calculated from the correlation functions by the method of cumulants and subsequently the mean particle diameters (z value) were obtained using the Stokes–Einstein relationship, Eq. (4). Three liposome batches per sample were analyzed, and data from three contiguous runs of eight records each were collected during a 30-min period. The resultant 72 data values were used to perform statistical analysis. In order to perform a more detailed analysis, intensity distribution of particle sizes and number frequency distribution were calculated from the correlation functions using the NNLS exponential sampling method [26] modified by Hallett et al. [27]. The modified and improved method includes the use of triangular averaging of scattering factors [27].

3.7. Wide angle integrated light scattering (WAILS)

A fiber-optic-based spectrophotometer was used to obtain $I(Q)$ vs. Q data from DPPC vesicles and DPPC vesicles with *Candida rugosa* lipase suspensions. Sixty millilitres of liposomes (30 mg DPPC/ml buffer) were mixed with CRL aliquots (50–200 ml) and left in a water bath at 25 or 35°C for 15 min. Following the incubation time, the samples were diluted to 3 ml with 0.1 M succinate buffer, pH 5.0. At this point the concentrations of DPPC and CRL corresponded to the ones used for the DLS experiments. However, the samples needed further dilution (1:20) because their concentrations were too high for this apparatus; 3.15×10^{-5} M, and from 8.5×10^{-9} M to 3.45×10^{-8} M, were finally used for DPPC and CRL, respectively. A 2-ml sample was then mixed in a quartz cuvette and placed in a water bath and set at the appropriate experimental temperature by a quartz vat. After 5 min, a continuous wave, tunable argon ion Lexel (Model 95) laser set to a wavelength of 488 nm was focused on the sample. Sample scattered intensities were measured at 20 scattering angles from 16° to 160°. The data were collected and stored in the form of $I(Q)$ vs. Q via computer interface as previosly described by Strawbridge et al. [34]. Calibration of the instrument was performed using 96 nm diameter latex spheres (Duke Scientific Corp., Palo Alto, CA, USA). Data from three different liposome batches were obtained at temperatures of 25 and 35°C. Liposomes were modeled as coated spheres with a coat thickness of 0.007 mm (assuming the vesicles to be unilamellar [28]), a coat refractive index of 1.45, lumen refractive index of 1.33, and the surrounding medium refractive index of 1.33. With the ILS distribution program, number distributions were calculated using RGD theory [28]. Other statistical analyses were performed using Graphpad Prism (Graphpad Software Inc., San Diego, CA, USA).

3.8. Statistical analysis

Statistical analyses were performed with SAS TM software for Windows TM release 6.12, unless otherwise stated. The designs were factorial in nature. To compare different studied conditions for each technique, data were treated using analysis of variance (ANOVA). Whenever the designs were unbalanced, the general linear model procedure (PROC GLM) was used instead of PROC ANOVA. To determine differences between levels, least significant difference test (LSD) (number of levels ≤ 6) and Duncan's multiple-range test (number of levels > 6) were used.

4. Results and discussion

4.1. Dynamic light scattering

Plots of changes (Δ) in vesicle diameter (vesicle diameter at a particular enzyme concentration-vesicle diameter in absence of enzyme) vs. enzyme concentration obtained by the addition of increasing amounts of CRL to DPPC liposomes, were used for the qualitative assessment of binding. For each condition studied, binding was detected by an increase in mean particle diameter upon the addition of increasing amounts of CRL.

The average size of DPPC vesicles extruded through 100 and 200 nm pore filters was 114 nm (S.D. = 3 nm) and 180 nm (S.D. = 30 nm) , respectively. Binding of *Candida rugosa* lipase to DPPC vesicles of both sizes was observed and no difference in binding behaviour was detected between the two.

In the absence of CRL at pH 5.0 and 35°C, the initial average vesicle sizes at 0, 0.2 and 1.0 M NaCl were 158.8, 164.1, and 177.8 nm, respectively. At pH 7.5 and 35°C, the initial average vesicle sizes at 0, 0.2 and 1.0 M NaCl were 144.0, 169.3 and 179.5 nm, respectively. Vesicle sizes increased with increases in NaCl concentration. The differences in vesicle size in the absence of CRL and in the presence of various NaCl concentrations may have been caused by either the change in the viscosity of the systems or the change in the 'optical' density of water, caused by Na^+ ions. In negatively charged vesicles it has been observed that Na^+ ions can change the density of the water located around the vesicle by as much as 10%, which, in turn, affects vesicle scattering properties (R. Hallett, personal communication). Although the effect of the Na^+ ions on zwitterionic vesicles is not known, a similar change in the density of the water could be expected.

Strong enzyme–vesicle interactions were evident when the medium contained salt. At pH 5.0 a significant difference ($P \leq 0.05$) in the liposome–protein interaction at the three different NaCl concentrations, 0, 0.2 and 1.0 M was detected. At pH 5.0, lipase–liposome interactions increased as a function of increasing NaCl concentration (Fig. 1a). At pH 7.5, a significant increase ($P < 0.05$) in lipase–liposome interactions was observed between 0 and 0.2 M NaCl, however, no significant differences were detected between 0.2 and 1.0 M NaCl ($P > 0.05$) (Fig. 1b). These results suggest that charge dispersion on the liposome and protein surface would facilitate CRL–liposome interactions by decreasing repulsive electrostatic charge interactions between the lipase and the liposome.

All the experiments performed by DLS were simultaneously run at pH 7.5 and pH 5.0, the

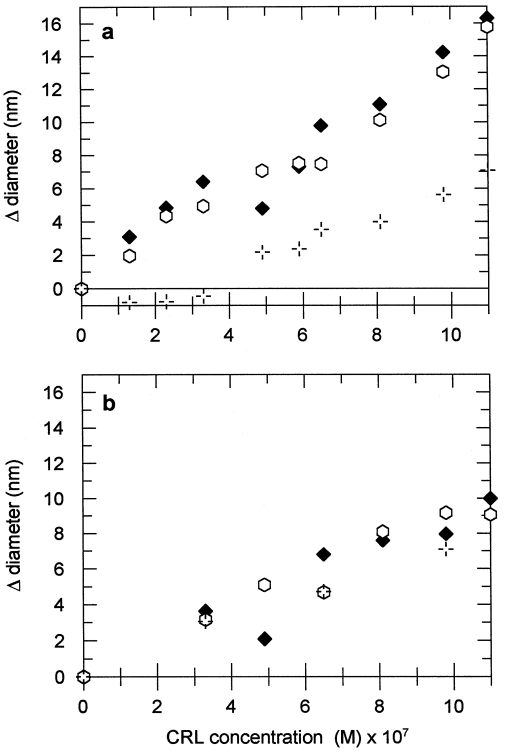

Fig. 1. Binding of *Candida rugosa* lipase to DPPC liposomes in 0.1 M succinate (a = pH 5.0, b = pH 7.5) and NaCl concentrations of (+) 0 M, (○) 0.2 M, and (◆) 1.0 M at 35°C. $n = 2$.

enzyme isoelectric point [35]. In a medium without NaCl, a significant difference in binding ($P \leq 0.05$) at the two pH values was detected. Lipase–liposome interactions were greater at pH 7.5. In a medium with 0.2 M NaCl no significant differences in binding between pHs were detected. DPPC is a zwitterionic, but electrically neutral phospholipid and CRL is a polyelectrolyte with a considerable number of charges; therefore, at pH 5.0 the enzyme was electrically neutral, while at pH 7.5 the enzyme was negatively charged. The presence of a negatively charged enzyme may have facilitated the interaction with the ammonium groups of the DPPC molecules in the liposomes which translated to better binding. These results suggest the participation of attractive electrostatic interactions in the process; however, the more favorable binding observed in the presence of salt would suggest that electrostatic

repulsions would have to be overcome before the lipase binds to the interface. A satisfactory explanation for this apparent contradiction could not be found.

In either situation, participation of electrostatic interactions in the process are evident. Other authors have reported on the involvement of electrostatic interactions in lipase–substrate binding. Geluk et al. [36] studied the role of electrostatic interactions in *Candida rugosa* lipase adsorption to microcrystalline cellulose. They showed that at the isoelectric pH, electrostatic interactions between the enzyme and a charged interface were minimized, suggesting that an electrostatic energy barrier had to be initially surmounted in order for the lipase to be adsorbed to a negatively charged interface. In 1993, Marangoni [22] reported that *Rhizopus arrhizus* lipase with a negative electric potential did not bind to DOPG liposomes, which have negatively charged head groups, but did bind to DPPC vesicles, which are electrically neutral. These findings suggest that initial binding of *Rhizopus arrhizus* lipase to DPPC interfaces is strongly influenced by electrostatic interactions.

There was a significant difference in CRL binding to DPPC liposomes among the three temperatures studied ($P \leq 0.0001$). In Fig. 2, binding curves at pH 5.0 and pH 7.5 and 25, 35 and 45°C in the absence of added NaCl are presented.

At 25°C very erratic liposome diameter change vs. CRL concentration curves were obtained. At the same time, polydispersity values for liposome samples at that temperature were very high, two or three times the values at the other temperatures, (data not presented). Other authors have obtained similar results. Biltonen et al. [37] found that PC liposomes in the gel-state are poor substrates for phospholipase A_2 and show anomalous kinetic patterns during hydrolysis and catalysis. The reason for this could be that at 25°C, DPPC was in the gel state which favored lipid–lipid interactions leading to aggregation. Lipase–liposome interactions were diminished because liposome aggregation resulted in a decreased number of liposome binding sites available for the enzyme to bind. Also, enzyme binding was more difficult because the process possibly required the presence of interface defects. Imperfections occurring

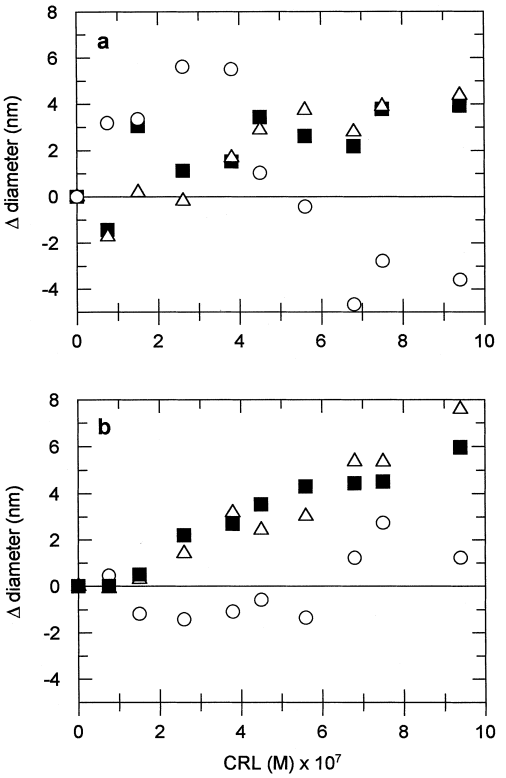

Fig. 2. Binding of *Candida rugosa* lipase to DPPC liposomes in 0 M NaCl, 0.1 M succinate, pH 5.0, at (○) 25°C, (△) 35°C, and (■) 45°C. $n = 2$.

between the molecular packing of the ordered and fluid domains appear only at and above the subtransition temperature [38,39]. This would facilitate a close contact of the enzyme with the interface.

At 35°C and 45°C CRL–liposome interactions were stronger than at 25°C. This indicates that hydrophobic forces may be involved in CRL–liposome interactions. The enthalpy change (ΔH) is greater than 0 when two or more solvated hydrophobic groups associate. Therefore, increases in temperature, in a range where ΔH remains positive, tend to drive the equilibrium toward hydrophobic bonding.

Considering the van't Hoff equation,

$$\frac{\mathrm{d}\ln K}{\mathrm{d}T} = \frac{\Delta H}{RT^2} \tag{13}$$

and solving for the equilibrium constant, K:

$$K = \exp(-\Delta H/RT) \quad (14)$$

where R is the gas constant and T is the absolute temperature. In Eq. (14), when ΔH is positive, the exponential term is always negative. As T increases, the exponential term gets smaller and K gets larger. Thus, there is a greater tendency for the bound form to exist [40].

Another factor that may have favored CRL–liposome interactions at the higher temperatures studied was the increase in the area per molecule (A_m) at the lipid–water interface of DPPC at the gel-to-liquid transition. With DPPC this transition can result in a change in A_m from 40 Å^2 below the temperature that marks the beginning of the phase transition, T_c, to 60 Å^2 above T_c [41].

4.1.1. A more detailed analysis of DLS data — a word of caution

A more detailed analysis of DLS data was performed using methods and software developed by Hallett et al. [27]. Intensity distributions obtained by performing the inversion method of Hallett et al. [27] on DLS data from samples incubated at 25°C, were bimodal. Intensity distribution histograms showed two populations, one with sizes in the range 40–400 nm and a second one with particle diameter sizes from 400 to 5000 nm (Fig. 3). The latter possibly corresponds to liposome aggregates which are formed when DPPC is in the gel state (25°C). The average diameter of both populations considered together was 491 nm (S.D. = 27 nm). In contrast, when analyzing the same data by cumulants (z average), the presence of only one population was detected, high polydispersity values were recorded, and the

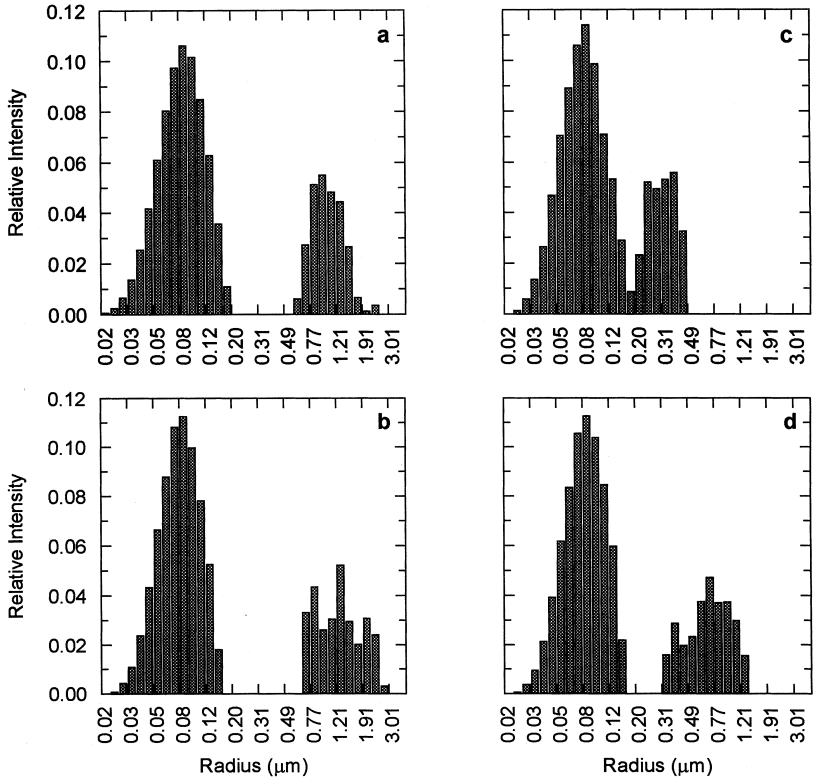

Fig. 3. Intensity distribution by DLS (obtained by performing an inversion method on DLS data) of binding of CRL: a. 0 M; b, 3.8×10^{-7} M; c, 5.6×10^{-7} M; and d, 6.8×10^{-7} M to DPPC liposomes in 0.2 M NaCl, 0.1 M succinate buffer (pH 5.0) at 25°C. $n = 2$.

average particle diameter was 240 nm (S.D. = 10 nm). These results suggest that the inversion method allowed for the detection of bimodality, otherwise undetected.

At 35°C and 45°C using the inversion method of Hallett et al. [27], bimodal distributions were also detected, but with smaller sizes than those observed at 25°C. At 35°C a small population with a mean diameter between 60 and 160 nm and a bigger one between 140 and 340 nm were observed. The latter corresponds to the liposomes. The average diameter was 188 nm (S.D. = 8 nm). On the other hand, *z* mean particle diameter was 179 nm (S.D. = 10 nm). At 45°C one population had a mean diameter between 60 and 140 nm and the other between 160 and 330 nm. The average diameter was 198 nm (S.D. = 2 nm) and *z* average particle diameter was 175 nm (S.D. = 9 nm).

Number distributions showed only the populations with the smallest diameter. This finding suggests that these populations were the ones present in higher numbers. Although the liposome preparations were extruded through filters of 200 nm, it is possible that micelles of small diameter were created. This happened with all the preparations under all conditions.

An illustration of intensity and number distribution histograms, where different concentrations of CRL were added to DPPC liposomes in 0.2 M NaCl, 0.1 M succinate buffer (pH 5.0) at 35°C, are shown in Fig. 4. Two populations were

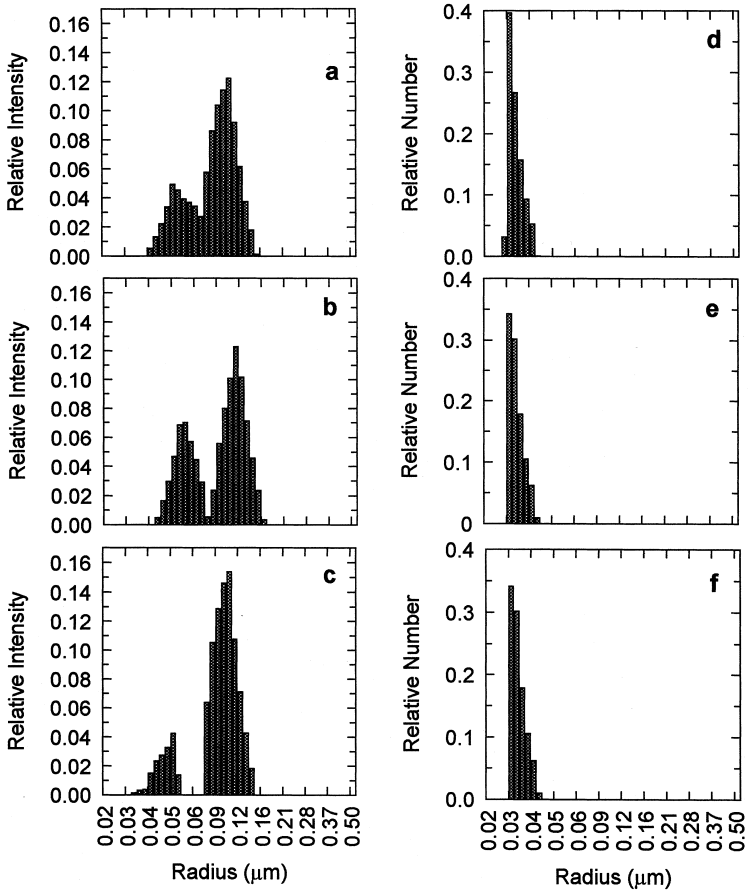

Fig. 4. Intensity and number distribution by DLS (obtained by performing an inversion method on DLS data) of binding of CRL a and d 0 M, b and e 4.5×10^{-7} M, c and f 7.5×10^{-7} M to DPPC liposomes in 0.2 M NaCl, 0.1 M succinate buffer (pH 5.0) at 35°C. $n = 2$.

detected, one with a mean diameter of 60 nm and the other, corresponding to the vesicles, with a mean diameter of 181 nm. After the addition of 7.5×10^{-7} M of CRL, mean vesicle diameter increased to 196 nm.

There was a discrepancy between the results obtained by DLS using different data analysis methods at 25°C. The inversion of the autocorrelation function $g^{(1)}(\tau)$ allowed for the detection of the various populations present in the system studied. On the other hand, cumulants analysis did not detect the population with the greatest diameters (aggregated liposomes). For this reason, the average particle size obtained using the inversion method of Hallett et al. [27] almost doubled the average obtained by cumulants. The erratic titration curves and the high data variability obtained at 25°C were a result of high polydispersity created by the presence of the aggregated liposomes.

At 35°C and 45°C, agreement did exist between the two methods of analysis due to the fact that at those temperatures vesicle aggregation did not occur. However, the inversion method of Hallett et al. [27] showed to be more appropriate for the enzyme–vesicle interaction analysis because it allowed for the differentiation of the two vesicle populations present in the system. On the other hand, cumulants analysis proved to be a useful tool in providing general trends of changes in liposome size (without population differentiation) due to enzyme–lipid interactions when neither vesicle aggregation (in the studied system at 25°C), nor multimodality occurred.

The combination of the two analyses produced useful results in our study for the detection of liposome aggregation, lipase–liposome binding, the presence of micelles, and the determination of general particle size distributions of the system. On the other hand, histograms of number distributions did not seem to be very useful in the study of lipase–liposome interactions because all the samples showed a very high, and unexpected, number of particles of small sizes.

4.2. WAILS

Addition of CRL to DPPC liposomes did not lead to an increase in mean vesicle diameter as determined by WAILS ($P > 0.05$). On the other hand, mean particle diameter size was significantly different at the two temperatures studied ($P < 0.05$) (Fig. 5).

The $I(Q)$ vs. Q plot of the CRL–DPPC liposomes interaction at 25°C showed that there were no differences in mean particle size when increasing concentrations of CRL were added. The histogram obtained from the data fit revealed the presence of a multimodal distribution with populations of particles in the diameter size range 150–360 nm, 260–1000 nm, and a tail in the diameter size range 1200–1800 nm (Fig. 6). The mean particle diameter size for suspensions of liposomes with and without enzyme was 496 nm (S.D. = 48 nm). This value agrees with the mean particle diameter size for suspensions of liposomes with and without enzyme obtained with the inversion method of Hallett et al. [27] (491 nm (S.D. = 27 nm)). With the latter, bimodality was shown by the intensity distribution histogram.

At 35°C no significant differences were found among the resultant mean particle diameters after the addition of increasing concentrations of CRL. In this case, a bimodal distribution was detected. The histogram showed one population of particles in the diameter size range 80–250 nm and another in the range 210–600 nm (Fig. 7).

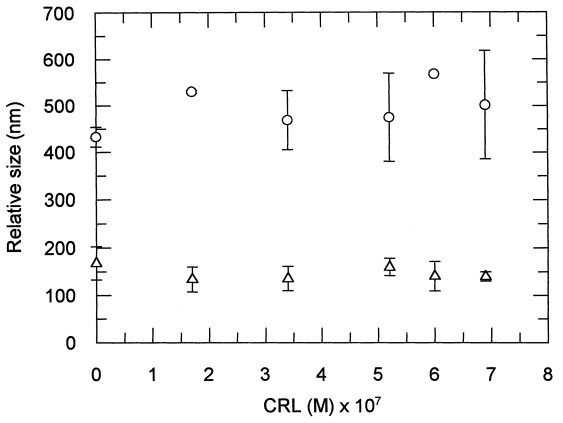

Fig. 5. DPPC liposomes relative size (nm) after the addition of different amounts of CRL at (○) 25°C, and (△) 35°C, by Wide Angle Integrated Light Scattering (WAILS). Error bars represent standard deviations ($n = 3$).

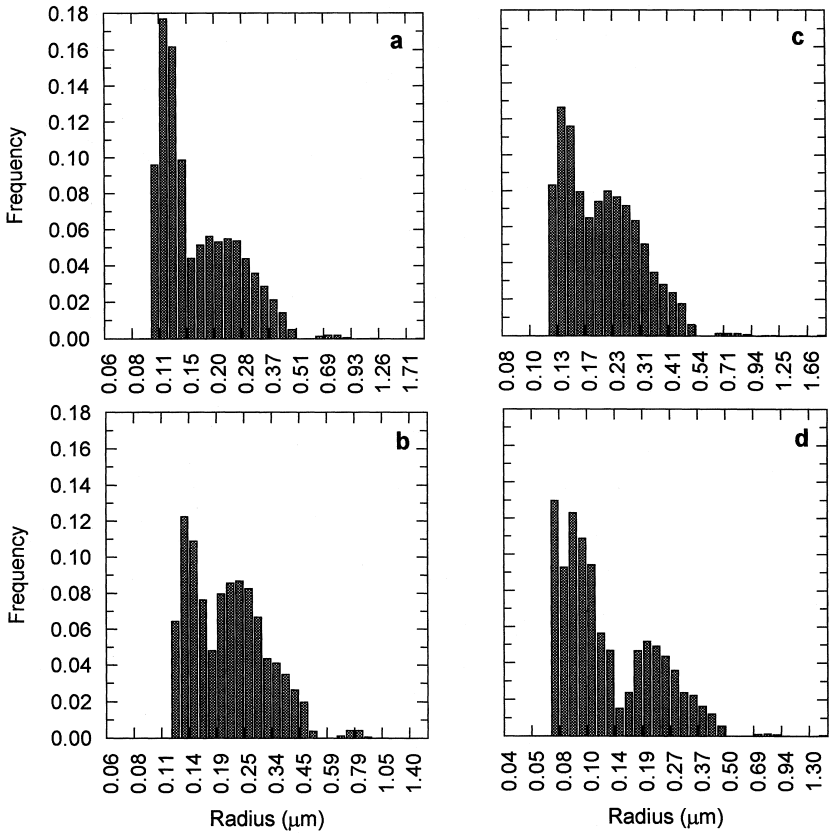

Fig. 6. Number distribution histograms obtained by WAILS. CRL a, 0 M; b, 1.7×10^{-7} M; c, 3.4×10^{-7} M; and d, 5.2×10^{-7} M was added to DPPC liposomes in 0.1 M succinate buffer (pH 5.0), at 25°C. $n = 1$.

The mean particle diameter for suspensions of liposomes with and without enzyme was 146 nm (S.D. = 14 nm). Analysis of DLS data by the inversion method of Hallett et al. [27] showed also bimodality and a slightly bigger average diameter 188 nm (S.D. = 8 nm).

Detection of particle diameters of more than 300 nm by intensity distribution obtained by the inversion method of Hallett et al. [27] and WAILS histograms confirmed the presence of liposome aggregates at 25°C. The congruence in the detection of different particle populations between the inversion method of Hallett et al. [27] and the discrete NNLS inversion method used in WAILS was due to the fact that they are similar mathematical inversion procedures of Eq. (3), and of Eq. (10) for DLS and WAILS, respectively, to obtain particle size distributions. At this temperature, mean particle size obtained by cumulants was erroneous because the greatest diameter population present in the system was undetected. On the other hand, mean particle sizes obtained by DLS using the inversion method of Hallett et al. [27] and WAILS were not useful for the present study because they included all the populations (liposome aggregates, micelles, enzyme, liposomes, enzyme–liposomes) and to analyze binding, liposome size has to be monitored separately. Therefore, histograms were the best choice for the data analysis.

The reasons for the smaller mean particle diameter size obtained by WAILS compared to DLS (using the inversion method of Hallett et al. [19]) at 35°C could be that DLS measures hydrodynamic radius, which is larger than the absolute particle size, and does not require calibration, as

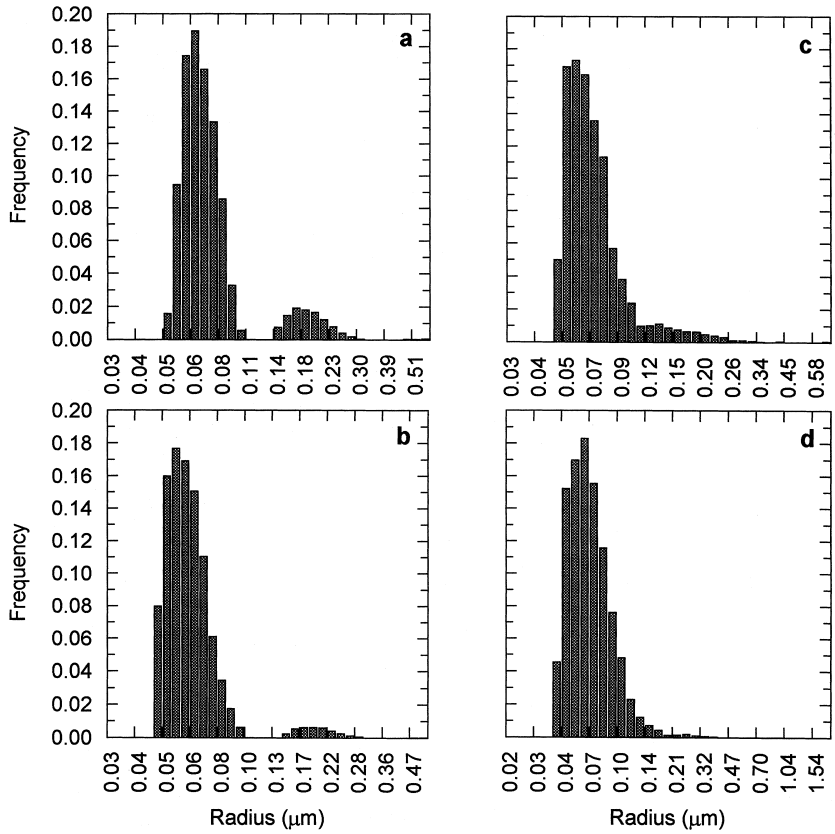

Fig. 7. Number distribution histograms obtained by WAILS. CRL a, 0 M; b. 1.7×10^{-7} M; c, 5.2×10^{-7} M; and d, 6.0×10^{-7} M, was added to DPPC liposomes in 0.1 M succinate buffer (pH 5.0), at 35°C. $n = 1$.

WAILS does. The diameter obtained by WAILS depends on the accuracy of a calibration with latex spheres of known diameter [28,21]. The maximum error from WAILS calibration effects is 10% and from noise in the signal is only 1% [28].

WAILS showed that the particles of diameter sizes in the range 150–360 nm and 80–250 nm for 25°C and 35°C, respectively (mainly liposomes) constituted the predominant population. In contrast, number distributions histograms by DLS showed very narrow size distributions for all the studied conditions (50–80 nm), indicating that small micelles were the population present in higher number. The discrepancy between results obtained by WAILS and DLS can be due to the failure of WAILS ($\lambda = 488$ nm) to detect particles smaller than ~ 100 nm. Other factors that could have caused the differences are the data acquisition procedure and the size distribution analysis. In DLS, statistical errors were correlated while in WAILS the experimental noise at each angle was independent [28]. Regarding the data analysis, data were fitted to Bessel functions by WAILS but to exponentials by DLS.

The difference between DLS and WAILS number distribution results could also be attributed to data collection times. For all DLS experiments runs of 30 min were performed. A trial at two conditions was conducted for run-times of 4 h, but no significant difference was detected between 30 min and 4 h runs. However, WAILS is number-weighted and the results obtained by this technique were more reasonable than the number distributions obtained by DLS. Moreover, the requirement of long data acquisition times (of several hours, perhaps 24 h periods) in order to

obtain accurate size distributions by DLS has already been reported [20].

5. Conclusions

Calculations of particle size by DLS are usually performed by cumulants analysis which produce a mean *z* average value. Enzyme–liposome systems are mainly multimodal. The multimodality of binding systems demands the use of data analysis methods other than cumulants. If cumulants analysis is used, care should be taken when interpreting binding results. Cumulants analysis proved to be useful in providing a general trend of liposome size change during enzyme–lipid interactions when neither vesicle aggregation, nor multimodality occurred. The use of a mathematical inversion on DLS data (method of Hallett et al. [27]) allows for the detection of different populations present in the system, making it possible to follow changes in particle size of individual populations. Intensity distributions obtained by the use of the inversion method of Hallett et al. [27] at 25°C and 35°C on DLS data are comparable with results obtained by WAILS using a similar inversion method. However, the present research suggests that data acquisition times equal or shorter than 4 h are not sufficient to produce reliable number distributions by DLS. WAILS emerged as the light scattering technique of preference for the study of lipase–liposome interaction investigations. WAILS is a fast and very sensitive technique, that allows the detection of different populations and directly produce accurate number distributions.

References

[1] G. Carta, J.L. Gainer, A.H. Benton, Enzymatic synthesis of esters using an immobilized lipase, Biotechnol. Bioeng. 37 (1991) 1004–1009.
[2] P.Y. Chen, S.H. Wu, K.T. Wang, Double enantioselective esterification of racemic acids and alcohols by lipase from *Candida cylindracea*, Biotechnol. Lett. 15 (1993) 181–184.
[3] S. Chattopadhyay, V.R. Mamdapur, Enzymatic esterification of 3-hydroxybutyric acid, Biotechnol. Lett. 14 (1993) 245–250.
[4] M. de Renobales, A.J.M. Lascaray, J.C. Mugica, L.C. Landeta, R. Solozabal, Hydrolysis of animal fats by lipase at temperatures below their melting points, Biotechnol. Lett. 14 (1992) 683–688.
[5] Y. Tanaka, T. Funada, J. Hirano, R. Hashizume, Triglyceride specificity of *Candida cylindracea* lipase: effect of docosahexanoic acid on resistance to triglyceride lipase, JAOCS 70 (1993) 1031–1034.
[6] E. Verger, Enzyme kinetics of lipolysis, in: S.P. Colowick, N.O. Kaplan (Eds.), Methods Enzymology, 64, Academic Press, New York, 1980, p. 340.
[7] C.A. Tan, M.F. Roberts, Engineering of the nonspecific phospholipase C from *Bacillus cereus*: replacement of glutamic acid-4 by alanine results in loss of interfacial catalysis and enhanced phosphomonoesterase activity, Biochemistry 37 (1998) 4275–4279.
[8] R. Verger, G.H. de Haas, Interfacial enzyme kinetics of lipolysis, Ann. Rev. Biophys. Bioeng. 5 (1976) 77–117.
[9] J.J. Volwerk, G.H. de Haas, Pancreatic phospholipase A2: a model for membrane-bound enzymes?, in: P.C. Jost, O.H. Griffith (Eds.), Lipid–protein interactions, 24, John Wiley and Sons, Toronto, 1982, p. 70.
[10] R. Verger, M.C.E. Mieras, G.H. de Haas, Action of phospholipase A at interfaces, J. Biol. Chem. 248 (1973) 4023–4034.
[11] P. Desnuelle, L. Sarda, G. Ailhaud, Inhibition de la lipasa pancréatique par le diéthyl-*p*-nitrophenyl phosphate en emulsion, Biochim. Biophys. Acta 37 (1960) 570–571.
[12] H. Brockerhoff, A model of pancreatic lipase and the orientation of enzymes at interfaces, Chem. Phys. Lipids 10 (1973) 215–222.
[13] W.K. Surewicz, R.M. Epand, Role of peptide structure in lipid–peptide interactions: a fluorescence study of the binding of pentagastrin-related pentapeptides to phospholipid vesicles, Biochemistry 23 (1984) 6072–6077.
[14] R.A. Parente, L. Nadasdi, N.K. Subbarao, F.C. Szoka, Jr., Association of a pH-sensitive peptide with membrane vesicles: role of amino acid sequence, Biochemistry 29 (1990) 8713–8719.
[15] M.K. Jain, M.R. Egmond, H.M. Verheij, R. Apitz-Castro, R. Dijkman, G.H. DeHaas, Interaction of phospholipase A_2 and phospholipid bilayers, Biochim. Biophys. Acta 688 (1982) 341–348.
[16] L.R. McLean, R.L. Jackson, Interaction of lipoprotein lipase and apolipoprotein C-II with sonicated vesicles of 1,2-ditetradecylphosphatidylcholine: comparison of binding constants, Biochemistry 24 (1985) 4196–4201.
[17] P.S. Araujo, M.Y. Rosseneu, J.M.H. Kremer, E.J.J. van Zoelen, G.H. de Haas, Structure and thermodynamic properties of the complexes between phospholipase A_2 and lipid micelles, Biochemistry 18 (1979) 580–586.
[18] G.M.D. Op Den Kelder, J.D.R. Hille, R. Dijkman, G.H. De Haas, M.R. Egmond, Binding of porcine pancreatic phospholipase A_2 to various micellar substrate analogues. Involvement of histidine-48 and aspartic acid-49 in the binding process, Biochemistry 20 (1981) 4074–4078.
[19] M.F. Roberts, A.D. Raymond, E.A. Dennis, Dual role of

interfacial phospholipid in phospholipase A_2 catalysis, Proc. Natl. Acad. Sci. USA 74 (1977) 1950–1954.
[20] K.B. Strawbridge, L.R. Palmer, A.R. Merril, F.R. Hallett, Integrated light-scattering spectroscopy, a sensitive probe for peptide–vesicle binding: application to the membrane-bound colicin E1 channel peptide, Biophys. J. 68 (1995) 131–136.
[21] E.W.J. Mosmuller, E.H.W. Pap, A.J.W.G. Visser, J.F.J. Engbersen, Steady-state fluorescence studies on lipase–vesicle interactions, Biochim. Biophys. Acta 1189 (1994) 45–51.
[22] A.G. Marangoni, Studies on the interaction of *Rhizopus arrhizus* lipase with dipalmitoylphosphatidylcholine liposomes, Colloids Surf. B: Biointerfaces 1 (1993) 167–176.
[23] D.G. Dalgleish, F.R. Hallett, Dynamic light scattering: applications to food systems, Food Res. Int. 28 (1995) 181–193.
[24] D.E. Koppel, Analysis of macromolecular polydispersity in intensity correlation spectroscopy — methods of cumulants, J. Chem. Phys. 57 (1972) 4814–4820.
[25] E.R. Pike, D. Watson, F.M. Watson, Analysis of polydisperse scattering data, in: B.E. Dahneke (Ed.), Measurements of Suspended Particles by Quasi-elastic Light Scattering, Wiley, New York, 1983, p. 107.
[26] I.D. Morrison, E.F. Grabowski, C.A.A. Herb, Improved techniques for particle size determination by quasi-elastic light scattering, Langmuir 1 (1985) 496–501.
[27] F.R. Hallett, T. Craig, J. Marsh, B. Nickel, Particle size analysis: number distributions by dynamic light scattering, Food Res. Int. 34 (1989) 63–70.
[28] K.B Strawbridge, F.R. Hallett, Size distributions obtained from the inversion of I(Q) using integrated light scattering, Macromolecular 27 (1994) 2283–2290.
[29] R. Nayar, M.J. Hope, P.R. Cullis, Generation of large unilamellar vesicles from long-chain saturated phosphatidylcholines by extrusion technique, Biochim. Biophys. Acta 986 (1989) 200–206.
[30] G.R. Bartlett, Phosphorus assay in column chromatography, J. Biol. Chem. 234 (1959) 466–468.
[31] K. Veeraragavan, B.F. Gibbs, Detection and partial purification of two lipases from *Candida rugosa*, Biotechnol. Lett. 11 (1989) 345–348.
[32] M. Bradford, Rapid and sensitive method for the quantitation of microgram quantities of proteins utilizing the principle of protein–dye binding, Anal. Biochem. 72 (1976) 248–254.
[33] D.Y. Kwon, J.S. Rhee, A simple and rapid colorimetric method for determination of free fatty acids for lipase assay, JAOCS 63 (1986) 89–92.
[34] K.B. Strawbridge, F.R. Hallett, J. Watton, Rapid determination of I(Q) using a fibre-optic based integrated light scattering spectrometer, Can. J. Appl. Spectroscopy 36 (1991) 53–60.
[35] M.L. Rúa, T. Díaz-Mauriño, V.M. Fernández, C. Otero, A. Ballesteros, Purification and characterization of two distinct lipases from *Candida cylindracea*, Biochim. Biophys. Acta 1156 (1993) 181–189.
[36] M.A. Geluk, W. Norde, H.K.A.I. Van Kalsbeek, K. Van't Riet, Adsorption of lipase from *Candida rugosa* on cellulose and its influence on lipolytic activity, Enzyme Microbiol. Technol. 14 (1992) 748–754.
[37] R.L. Biltonen, T.R. Heimburg, B.K. Lathrop, J.D. Bell, Molecular aspects of phospholipase A_2 activation, Adv. Exp. Med. Biol. 279 (1990) 85–103.
[38] M.D. Houslay, K.K. Stanley, Dynamics of Biological Membranes, Influence on Synthesis, Structure and Function, John Wiley and Sons Ltd, Toronto, 1982.
[39] M.K. Jain, J. Rogers, L. Simpson, L.M. Gierasch, Effect of tryptophan derivatives on the phase properties of bilayers, Biochim. Biophys. Acta 816 (1985) 153–162.
[40] C.R. Cantor, P.R. Schimmel, Biophysical Chemistry Part I, The Conformation of Biological Macromolecules, Freeman and Co, New York, 1980.
[41] P.L. Yeagle, The Membranes of Cells, Academic Press, San Diego, 1993.